COMPRESSED SENSING RECONSTRUCTION OF DYNAMIC CONTRAST ENHANCED MRI USING GPU-ACCELERATED CONVOLUTIONAL SPARSE CODING

Tran Minh Quan and Won-Ki Jeong

School of Electrical and Computer Engineering,
Ulsan National Institute of Science and Technology (UNIST), Ulsan, South Korea
E-mail: {quantm, wkjeong}@unist.ac.kr

ABSTRACT

In this paper, we propose a data-driven image reconstruction algorithm that specifically aims to reconstruct undersampled dynamic contrast enhanced (DCE) MRI data. The proposed method is based on the convolutional sparse coding algorithm, which leverages the Fourier convolution theorem to accelerate the process of learning a collections of filters and iteratively refines the reconstruction result using the sparse codes found during the reconstruction process. We introduce a novel energy formation based on the learning over time-varing DCE-MRI images, and propose an extension of Alternating Direction Method of Multiplier (ADMM) method to solve the constrained optimization problem efficiently using the GPU. We assess the performance of the proposed method by comparing with the state-of-the-art dictionary-based compressed sensing (CS) MRI method.

Index Terms— Convolutional Sparse Coding, Compressed Sensing, MRI, GPU.

1. INTRODUCTION

One of the main problems hinders adopting MRI for time-critical application is its longer acquisition time. There has been much research effort to accelerate MRI acquisition process using hardware and software. Among them, compressed sensing has been successfully endorsed as a software approach to reconstruct high-quality images from undersampled raw MRI data (i.e., k-space data). Since CS-MRI imposes an additional computation burden and suffers from reconstruction artifact, CS-MRI research has mostly focused on developing faster numerical algorithms and improving image quality for low sampling rates.

The earlier CS-MRI work mainly focused on the ℓ_1-norm energy minimization problem over sparse signal generated using universal sparsifying transforms, such as Total Variation, Wavelet, and Fourier transform, as introduced in the seminal work by Lustig et al. [1]. Even though such methods may be relatively fast due to their simplicity, the image quality may not be optimal because such universal transforms may not represent various local image features effectively. GPU-acceleration has also been well-adopted to reduce the computing time of such algorithms [2].

On the other hand, recent data-driven approaches, such as dictionary learning [3], are adopted to CS-MRI reconstruction and showed significant improvement in image quality [4]. The main novelty of this approach is to derive a sparsifying transform via a machine learning process, which accurately represent local features of reconstructed image compared to those of universal transforms. However, a drawback of this approach is its computational cost because patch-based dictionary learning is a highly time-consuming process. A recent advance in dictionary learning, convolutional sparse coding [5], replaces the patch-based dictionary learning process with an energy minimization process using a convolution operator on the image domain, which leads to an element-wise multiplication in frequency domain, derived within ADMM framework [6]. Later, a more efficient method based on a direct inverse problem is proposed by Wohlberg [7]. However, such advanced machine learning approaches have not been fully exploited in CS-MRI literature yet.

In this paper, we introduce a novel application of convolutional sparse coding to reconstruct undersampled DCE-MRI. We leverage the property of DCE-MRI that many similar local features may appear over time due to its temporal coherency so that learning a dictionary from the images over the range of time can improve the reconstruction quality better than using the temporal Total Variation energy only. In contrast to the conventional dictionary learning-based CS-MRI [4], our method can avoid expensive patch-based learning by embedding the convolution operator directly into the energy function and its solution can be efficiently computed in the frequency domain, i.e., k-space, using an alternating method. We also show that the proposed method maps well to data-parallel architecture, such as GPUs, for further accelerating its running time significantly. To the best of our knowledge, this is the first CS-DCE-MRI reconstruction method based on convolutional sparse coding and GPU acceleration.

2. METHOD

Figure 1 is a pictorial description of the proposed method. If the inverse Fourier transform is directly applied to undersampled DCE-MRI k-space data (Fig. 1a, $\times 8$ undersampling), the reconstructed images will suffer from artifacts (Fig. 1b). The zero-filling reconstruction shown above will serve as an initial guess (Fig. 1c) for our iterative reconstruction process with randomly initialized filters, e.g., a collection of 100 atoms of

978-1-4799-2349-6/16/$31.00 ©2016 IEEE

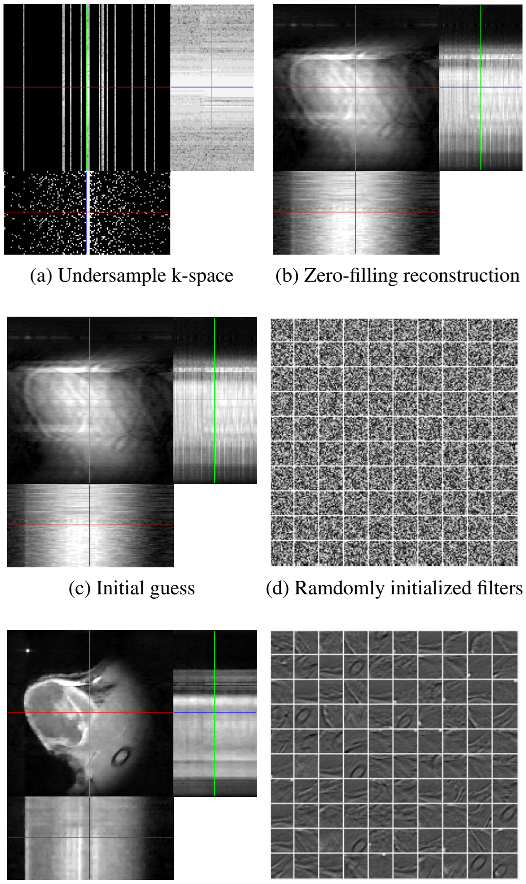

(a) Undersample k-space (b) Zero-filling reconstruction

(c) Initial guess (d) Ramdomly initialized filters

(e) Converged solution (f) Converged filters

Fig. 1: CS-DCE-MRI Reconstruction using convolutional sparse coding. Red line: t axis, Blue–green lines: x–y axis

size 21×21 as shown in Fig. 1d. Then the image and filters are iteratively updated until they converge as shown in Fig. 1e and f. The proposed CS-DCE-MRI reconstruction algorithm is a process of finding S_i (i.e., DCE MR image at the time step i) of the energy minimization problem defined as follows:

$$\min_{D_k, X_{k,i}, S_i} \frac{\alpha}{2} \left\| \sum_k D_k * X_{k,i} - S_i \right\|_2^2 + \lambda \sum_k \|X_{k,i}\|_1 + \theta \|\nabla_t S_i\|_1$$
$$s.t. \quad \|R_i \mathcal{F} S_i - M_i\|_2^2 < \varepsilon, \|D_k\|_2^2 \leq 1 \tag{1}$$

where D_k is the k-th filter (or atom in the dictionary) and $X_{k,i}$ is its corresponding sparse code for S_i. In order to reconstruct the entire DCE MR images for t time steps, we should solve Eq (1) for $i = 0, ..., t-1$.

In Eq. (1), the first term measures the difference between S_i and its sparse approximation $\sum_k D_k * X_{k,i} - S_i$ weighted by α. The second term is the sparsity regularization of $X_{k,i}$ using an ℓ_1 norm with a weight λ instead of an ℓ_0 norm as used in [3; 4]. The third term $\theta\|\nabla_t S_i\|_1$ is the Total Variation energy that enforces the temporal coherence of DCE data, which is widely used in conventional CS-DCE-MRI reconstruction algorithms [1; 2]. The rest of the equation is the collection of constraints – the first constraint enforces the consistency between each undersampled measurement M_i and the undersampled reconstructed image using the mask R_i and the Fourier operator $\mathcal{F}$, and the second constraint restricts the Frobenius norm of each atom D_k within a unit length. In the following sections, we split Eq. (1) into two sub optimization problems and alternate between them to find the global minimum solution for $\mathbf{S} = \{S_0, S_1, ..., S_{t-1}\}$. In the following discussion, we will use a simplified notation without indices k and i and replace the result of Fourier transform of a given variable by using the subscript f (for example, S_f is the simplified notation for $\mathcal{F}S_i$) to derive the solution of Eq. (1).

2.1. Subproblem for convolutional sparse coding

The first sub optimization problem of Eq. (1) is the formulation of convolutional sparse coding as follows:

$$\min_{D,X,S} \quad \frac{\alpha}{2} \left\| \sum D * X - S \right\|_2^2 + \lambda \sum \|X\|_1$$
$$s.t. \; \|RS_f - M\|_2^2 < \varepsilon, \;\; \|D\|_2^2 \leq 1 \tag{2}$$

Problem (2) can be rewritten using auxiliary variables Y and G for X and D:

$$\min_{D,G,X,Y,S} \quad \frac{\alpha}{2} \left\| \sum D * X - S \right\|_2^2 + \lambda \sum \|Y\|_1$$
$$s.t. \; X = Y, \; \|RS_f - M\|_2^2 < \varepsilon, \; G = \mathcal{P}roj(D), \;\; \|G\|_2^2 \leq 1 \tag{3}$$

where G and D are related by a projection operator as a combination of a truncated matrix followed by a padding-zero matrix in order to make the dimension of G same as that of X. Since we will leverage Fourier transform to solve this problem, G should be padded to zero to make its size same as G_f and X_f. The above constraint problem can be rebuilt in an augmented Lagrangian form with dual variables U, H, and further regulates the measurement consistency and the dual differences with γ, ρ, and σ, respectively:

$$\min_{D,G,X,Y,S} \quad \frac{\alpha}{2} \left\| \sum D * X - S \right\|_2^2 + \frac{\gamma}{2} \|RS_f - M\|_2^2$$
$$+ \lambda \sum \|Y\|_1 + \frac{\rho}{2} \|X - Y + U\|_2^2 + \frac{\sigma}{2} \sum \|D - G + H\|_2^2$$
$$s.t. \quad G = \mathcal{P}roj(D), \quad \|G\|_2^2 \leq 1 \tag{4}$$

Then we can solve problem (4) by iteratively finding the solution of independent smaller problems, as described below:

Solve for X:

$$\min_X \frac{\alpha}{2} \left\| \sum D * X - S \right\|_2^2 + \frac{\rho}{2} \|X - Y + U\|_2^2 \tag{5}$$

If we apply the Fourier transform to the (5), it becomes:

$$\min_{X_f} \frac{\alpha}{2} \left\| \sum D_f X_f - S_f \right\|_2^2 + \frac{\rho}{2} \|X_f - Y_f + U_f\|_2^2 \tag{6}$$

Then the minimum solution of (6) can be found by taking the derivative of (6) with respect to X_f and setting it to zero as follows:

$$\left(\alpha \sum D_f^H D_f + \rho I \right) X_f = \alpha \sum D_f^H S_f + \rho \left(Y_f - U_f \right) \tag{7}$$

Solve for Y:

$$\min_Y \quad \lambda \sum \|Y\|_1 + \frac{\rho}{2} \|X - Y + U\|_2^2 \tag{8}$$

Y for ℓ_1 minimization problem can be found by using a shrinkage operation:

$$Y = \mathcal{S}hrink_{\lambda/\rho}\left(X + U\right) \tag{9}$$

Solve for U: The update rule for U can be defined as a fixed-point iteration with the difference between X and Y (U converges when X and Y converge each other) as follows:

$$U = U + (X - Y) \tag{10}$$

Solve for D: Similar to (7) , D can be solved in the Fourier domain:

$$\left(\alpha \sum X_f^H X_f + \sigma I\right) D_f = \alpha \sum X_f^H S_f + \sigma\left(G_f - H_f\right) \tag{11}$$

Solve for G: G can be found by taking the inverse Fourier transform of D_f. This projection should be constrained by suppressing the elements which are outside the filter size D_k, and followed by normalizing its ℓ_2-norm to a unit length.

$$\min_{G} \; \frac{\sigma}{2}\left\|D - G + H\right\|_2^2 \;\; s.t \;\; G = \mathcal{P}roj(D), \;\; \|G\|_2^2 \leq 1 \tag{12}$$

Solve for H: Similar to U, the update rule for H can be defined as follows:

$$H = H + (D - G) \tag{13}$$

Solve for S:

$$\min_{S} \; \frac{\alpha}{2}\left\|D * X - S\right\|_2^2 + \frac{\gamma}{2}\left\|RS_f - M\right\|_2^2 \; s.t. \; S_f = \mathcal{F}(S) \tag{14}$$

Similar to (6), the objective function of (14) can be transformed into Fourier domain:

$$\min_{S_f} \quad \frac{\alpha}{2}\left\|\sum D_f X_f - S_f\right\|_2^2 + \frac{\gamma}{2}\left\|RS_f - M\right\|_2^2 \tag{15}$$

Then S_f can be found by solving the following linear system:

$$\left(\gamma R^H R + \alpha I\right) S_f = \gamma R^H M + \alpha \sum D_f X_f \tag{16}$$

Note that the efficient solutions of (7), (11) and (16) can be obtained via the Sherman-Morrison formula for independent linear systems as shown in [7].

2.2. Subproblem for Total Variation along t

The second sub optimization problem of Eq (1) is the regularizer with a temporal Total Variation energy. In order to solve this problem, we need to minimize the following energy for the entire set of images $\mathbf{S} = \{S_0, S_1, ..., S_{t-1}\}$ collectively with the image consistency energy for the measurement $\mathbf{M} = \{M_0, M_1, ..., M_{t-1}\}$ and the sampling mask $\mathbf{R} = \{R_0, R_1, ..., R_{t-1}\}$ as shown below:

$$\min_{s} \theta \left\|\nabla_t \mathbf{S}\right\|_1 \quad s.t. \quad \left\|\mathbf{R}\mathcal{F}\mathbf{S} - \mathbf{M}\right\|_2^2 < \varepsilon \tag{17}$$

By introducing the auxiliary variable $\mathbf{P}$, the above problem becomes:

$$\min_{\mathbf{P}} \theta \left\|\mathbf{P}\right\|_1 \quad s.t. \quad \left\|\mathbf{R}\mathcal{F}\mathbf{S} - \mathbf{M}\right\|_2^2 < \varepsilon, \;\; \nabla_t \mathbf{S} = \mathbf{P} \tag{18}$$

By adding dual variable $\mathbf{Q}$, it results in an unconstrained problem as following:

$$\min_{\mathbf{S},\mathbf{P}} \theta \left\|\mathbf{P}\right\|_1 + \frac{\gamma}{2}\left\|\mathbf{R}\mathcal{F}\mathbf{S} - \mathbf{M}\right\|_2^2 + \frac{\delta}{2}\left\|\nabla_t \mathbf{S} - \mathbf{P} + \mathbf{Q}\right\|_2^2 \tag{19}$$

Solve for $\mathbf{P}$:

$$\min_{\mathbf{P}} \theta \left\|\mathbf{P}\right\|_1 + \frac{\delta}{2}\left\|\nabla_t \mathbf{S} - \mathbf{P} + \mathbf{Q}\right\|_2^2 \tag{20}$$

$$\mathbf{P} = \mathcal{S}hrink_{\theta/\delta}\left(\nabla_t \mathbf{S} + \mathbf{Q}\right) \tag{21}$$

Solve for $\mathbf{S}$:

$$\min_{\mathbf{S}} \frac{\gamma}{2}\left\|\mathbf{R}\mathcal{F}\mathbf{S} - \mathbf{M}\right\|_2^2 + \frac{\delta}{2}\left\|\nabla_t \mathbf{S} - \mathbf{P} + \mathbf{Q}\right\|_2^2 \tag{22}$$

$$\left(\gamma \mathcal{F}^H \mathbf{R}^H \mathbf{R}\mathcal{F} - \delta \Delta_t\right) \mathbf{S} = \gamma \mathcal{F}^H \mathbf{R}^H \mathbf{M} + \delta \nabla_t^H \left(\mathbf{P} - \mathbf{Q}\right) \tag{23}$$

Since the dimension of operator $\mathcal{F}$ is 2D but that of Δ_t is 1D, an efficient update rule for $\mathbf{S}$ can be obtained using a single iteration method as shown in [2].

Solve for $\mathbf{Q}$: The update rule for $\mathbf{Q}$ is defined using a fixed point iteration as follows:

$$\mathbf{Q} = \mathbf{Q} + \left(\nabla_t \mathbf{S} - \mathbf{P}\right) \tag{24}$$

Note that the dual variable $\mathbf{Q}$ and others (U, H) are equivalent to Bregman variables used in [2], in term of terminology.

3. RESULTS

In order to assess the performance of the proposed method, we ran our algorithm and [4] on four tumor DCE-MRI datasets. In the experiment, we used 2D atoms (i.e., filters) of size 16×16. The MRI datasets used in this experiment were perfusion dynamic tumor images processed with the Gd-DTPA agent to reconstruct the contrast profiles overtime. The CS-undersampling factor was set to ×8.

Convergence evaluation: As showed in Figure 2, the achieved Peak Signal-To-Noise-Ratios (PSNRs) of the proposed method are significantly higher than those of Caballero et al. [4]. In addition, our approach also converged faster to the steady stage on both datasets although our initial filter values are chosen randomly while Caballero et al. used the discrete cosine transform (DCT) basis at the beginning. The difference results are mainly from the numerical solver and the energy formulation.

Running time evaluation: The wall-clock running times are measured on a PC equipped with an Intel i7 CPU with 16 GB main memory and an NVIDIA GTX Geforce 980 Ti GPU. The prototype code is written in MATLAB 2015b including GPU implementation. As shown in Figure 3, we observed that our method is about 7× to 9× faster than the stage-of-the-art dictionary learning based CS-MRI reconstruction method [4] for 100 epochs (i.e., the number of learning iterations).

Quality evaluation: Figure 4 visualizes the first 64 (out of 256) atoms, the reconstructed images, and the errors compared to the full reconstruction, respectively. Our learning method can generate atoms that capture details of the image features much better than the patch-based learning method (Fig. 4a). Because the patch-based learning method generate smoother atoms (e.g., Gabor-like edges), the reconstruction

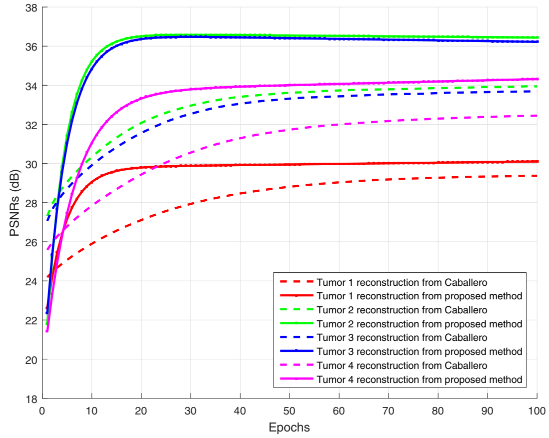

Fig. 2: Convergence rate evaluation based on PSNRs.

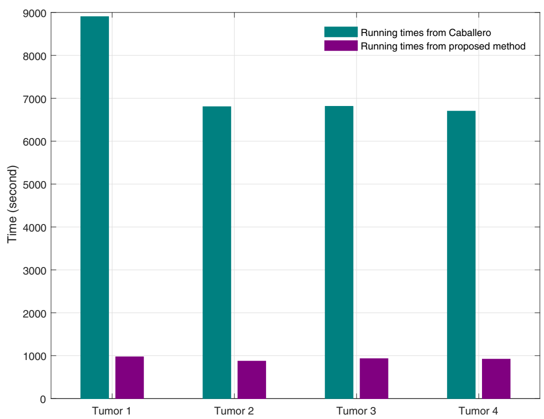

Fig. 3: Running times of 100 epochs.

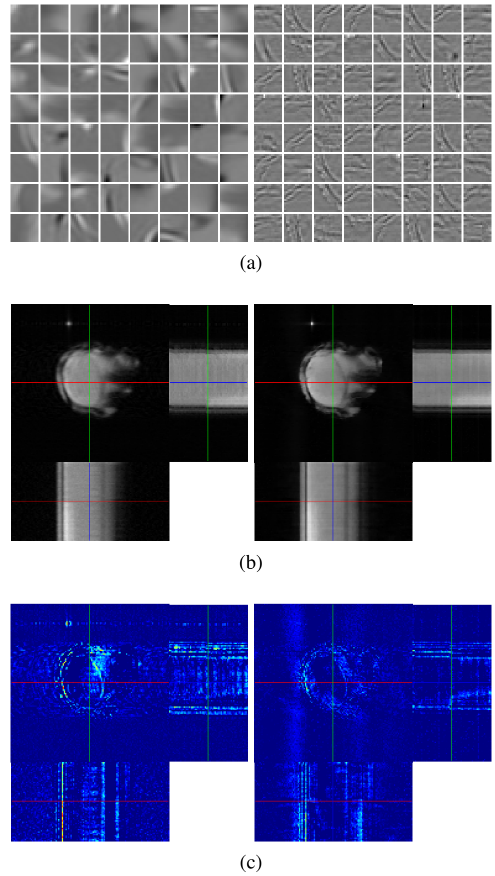

Fig. 4: Left: the patch-based dictionary learning method [4]. Right: the proposed method. (a) generated dictionaries, (b) reconstructed images, (c) error plots (red: high, blue: low).

process relies more on accurate sparse coding, which results in less-optimal convergence in the minimization process and higher error rates compared to our method.

4. CONCLUSION

In this paper, we introduced an efficient CS-MRI reconstruction method based on convolutional sparse coding and a temporal Total Variation regularizer. The proposed numerical solver is derived under the ADMM framework by leveraging the Fourier convolution theorem, which can be effectively accelerated using GPUs. As a result, we achieved faster convergence rate and higher PSNRs compared to the state-of-the-art CS-MRI reconstruction method using a patch-based dictionary learning. In the future, we plan to extend this method to include the temporal coherency directly on the atoms and assess its feasibility in clinical applications.

5. ACKNOWLEDGEMENTS

We would like to thank Sohyun Han and Hyungjoon Cho for sharing the DCE-MRI data. This research was supported by the Bio & Medical Technology Development Program of the National Research Foundation of Korea (NRF) funded by the Korean government, MSIP(NRF-2015M3A9A7029725), and the Basic Science Research Program through the NRF funded by the Ministry of Education (NRF-2014R1A1A2058773)

6. REFERENCES

[1] M. Lustig, D. Donoho, and J. M. Pauly, "Sparse MRI: the application of compressed sensing for rapid MR imaging," *Magnetic Resonance in Medicine*, vol. 58, no. 6, pp. 1182–1195, 2007.

[2] T. M. Quan, S. Han, H. Cho, and W.-K. Jeong, "Multi-GPU Reconstruction of Dynamic Compressed Sensing MRI," in *Medical image computing and computer-assisted intervention (MICCAI)*, no. 9351, pp. 484–492, 2015.

[3] M. Aharon, M. Elad, and A. Bruckstein, "K-SVD: An Algorithm for Designing Overcomplete Dictionaries for Sparse Representation," *IEEE Transactions on Signal Processing*, vol. 54, pp. 4311–4322, Nov. 2006.

[4] J. Caballero, A. Price, D. Rueckert, and J. Hajnal, "Dictionary Learning and Time Sparsity for Dynamic MR Data Reconstruction," *IEEE Transactions on Medical Imaging*, vol. 33, pp. 979–994, Apr. 2014.

[5] H. Bristow, A. Eriksson, and S. Lucey, "Fast Convolutional Sparse Coding," in *2013 IEEE Conference on Computer Vision and Pattern Recognition (CVPR)*, pp. 391–398, June 2013.

[6] C. S. Boyd, N. Parikh, E. Chu, B. Peleato, J. Eckstein, S. Boyd, N. Parikh, E. Chu, B. Peleato, and J. Eckstein, *Distributed Optimization and Statistical Learning via the Alternating Direction Method of Multipliers*. 2011.

[7] B. Wohlberg, "Efficient convolutional sparse coding," in *2014 IEEE International Conference on Acoustics, Speech and Signal Processing (ICASSP)*, pp. 7173–7177, May 2014.